Up-regulation of the manganese transporter SLC30A10 by hypoxia-inducible factors defines a homeostatic response to manganese toxicity

Chunyi Liu[a], Thomas Jursa[b], Michael Aschner[c], Donald R. Smith[b], and Somshuvra Mukhopadhyay[a,1]

[a]Division of Pharmacology & Toxicology, College of Pharmacy, Institute for Neuroscience, The University of Texas at Austin, Austin, TX 78712; [b]Department of Microbiology and Environmental Toxicology, University of California, Santa Cruz, CA 95064; and [c]Department of Molecular Pharmacology, Albert Einstein College of Medicine, Bronx, NY 10461

Manganese (Mn) is an essential metal that induces incurable parkinsonism at elevated levels. However, unlike other essential metals, mechanisms that regulate mammalian Mn homeostasis are poorly understood, which has limited therapeutic development. Here, we discovered that the exposure of mice to a translationally relevant oral Mn regimen up-regulated expression of SLC30A10, a critical Mn efflux transporter, in the liver and intestines. Mechanistic studies in cell culture, including primary human hepatocytes, revealed that 1) elevated Mn transcriptionally up-regulated SLC30A10, 2) a hypoxia response element in the *SLC30A10* promoter was necessary, 3) the transcriptional activities of hypoxia-inducible factor (HIF) 1 or HIF2 were required and sufficient for the SLC30A10 response, 4) elevated Mn activated HIF1/HIF2 by blocking the prolyl hydroxylation of HIF proteins necessary for their degradation, and 5) blocking the Mn-induced up-regulation of SLC30A10 increased intracellular Mn levels and enhanced Mn toxicity. Finally, prolyl hydroxylase inhibitors that stabilize HIF proteins and are in advanced clinical trials for other diseases reduced intracellular Mn levels and afforded cellular protection against Mn toxicity and also ameliorated the in vivo Mn-induced neuromotor deficits in mice. These findings define a fundamental homeostatic protective response to Mn toxicity—elevated Mn levels activate HIF1 and HIF2 to up-regulate SLC30A10, which in turn reduces cellular and organismal Mn levels, and further indicate that it may be possible to repurpose prolyl hydroxylase inhibitors for the management of Mn neurotoxicity.

metal | homeostasis | parkinsonism | HIF | ZnT10

Levels of essential metals (e.g., iron [Fe], copper [Cu], zinc [Zn], manganese [Mn], etc.) must be maintained within a narrow physiological range in cells and organisms to avoid deficiency or toxicity. For several essential metals, sophisticated homeostatic pathways that respond to changes in metal levels and adjust metal influx or efflux in a cell- or tissue-specific manner have been described. As examples, 1) the production of the liver hormone hepcidin increases during Fe overload, which induces degradation of the Fe efflux transporter ferroportin (Fpn) in Fe-exporting cells (e.g., enterocytes, macrophages, etc.) to inhibit the further release of Fe into plasma (1), and 2) the Cu efflux transporter ATP7B relocalizes from the *trans* Golgi network to cytoplasmic vesicles and the apical plasma membrane of hepatocytes to increase Cu excretion during excess (2). Predictably, dysfunctions in the pathways that regulate metal homeostasis often cause disease. Hepcidin deficiency causes hereditary hemochromatosis characterized by elevated Fe levels in the body (1), and ATP7B mutants that fail to traffic in response to Cu are associated with Wilson's disease and Cu toxicity (3, 4). Furthermore, insights obtained from studies on metal homeostasis have promoted drug discovery—for example, drugs that target the hepcidin–Fpn response are in clinical trials for the treatment of Fe metabolism diseases (5). Overall, elucidating the homeostatic control mechanisms that modulate levels of essential metals in human-relevant

model systems is essential to understand the pathobiology of, and develop treatments for, metal-induced diseases.

Unlike other essential metals, the regulation of Mn homeostasis is poorly understood. The only well-characterized molecular response to Mn in eukaryotes comes from studies in yeast—in this system, the Mn importers Smf1p and Smf2p are stabilized during Mn starvation and degraded under replete or toxic Mn levels (6, 7). However, protein levels of DMT1, the human homolog of yeast Smf1p/Smf2p, have not been reported to respond to changes in Mn levels. In mammalian systems, the understanding of Mn homeostasis is limited to insights obtained from elegant radiotracer Mn elimination and tissue distribution studies in rodents performed by Cotzias and coworkers in the 1950s and 1960s, which suggested that changes in Mn excretion are the primary means to control body Mn levels (8–10). However, although five decades have passed since these studies, the underlying molecular mechanisms remain unidentified.

Determining the homeostatic control mechanisms of Mn is biomedically important because of the toxicity of Mn in humans. Briefly, at elevated levels, Mn accumulates in the brain, primarily in the basal ganglia, and induces severe, incurable neurotoxicity that manifests as a parkinsonian-like movement disorder in adults

Significance

Manganese is an essential metal, but elevated levels cause incurable parkinsonism. A major limitation in treating manganese-induced parkinsonism is a lack of understanding of the mechanisms that regulate levels of manganese in the body. This manuscript defines a homeostatic regulatory pathway for manganese in mammalian systems. Elevated manganese levels increase expression of SLC30A10, a protein that mediates manganese excretion, thereby reducing the body burden of manganese. Findings also define the involved mechanisms by showing that manganese enhances SLC30A10 expression by activating the hypoxia-inducible factor transcription cascade. Finally, the study reveals that hypoxia-inducible factor stabilizing drugs reduce manganese levels to protect cells and mice against manganese toxicity, providing a means to treat manganese-induced parkinsonism in humans.

and neuromotor and executive function deficits in children (reviewed in ref. 11). Established causes of Mn neurotoxicity include elevated exposure from occupational sources in adults (e.g., welding, manufacture of batteries and steel, etc.) (11–13) or environmental sources in children and adolescents (e.g., drinking water) (14–24), defective excretion due to chronic liver disease (e.g., alcoholic cirrhosis) (25–31) because Mn is primarily excreted by the liver (10, 32–35), or, as described below, homozygous loss-of-function mutations in *SLC30A10* or *SLC39A14* (36–40). Mn neurotoxicity due to elevated exposure or liver dysfunction is associated with modest approximately one- to fivefold or approximately one- to sevenfold increases in brain Mn levels, respectively (11), implying that Mn rapidly becomes toxic as levels exceed the physiologic range (larger increases in tissue Mn levels occur in patients with *SLC30A10* or *SLC39A14* mutations). Furthermore, while Mn-induced parkinsonism is pathologically distinct from Parkinson's disease (41, 42), elevated Mn induces α-synuclein aggregation (43) and may enhance the risk of developing Parkinson's disease (44). In sum, Mn neurotoxicity is an important public health problem for which effective interventions are urgently required, and a mechanistic understanding of Mn homeostasis is expected to facilitate the development of viable therapeutic strategies.

Altered expression/activity of metal transporters is a primary mode of controlling metal homeostasis. However, until recently, transporters critical for Mn influx and efflux in humans were unknown, and this gap in knowledge hindered studies on Mn homeostasis. Needed breakthroughs came over the last few years when homozygous loss-of-function mutations in *SLC30A10* or *SLC39A14* were reported to increase Mn levels in the blood and brain and induce hereditary Mn neurotoxicity in humans (36–40), while homozygous loss-of-function mutations in *SLC39A8* were reported to lead to the onset of hereditary Mn deficiency (45, 46). We discovered that SLC30A10 is a cell surface–localized Mn efflux transporter that transports Mn from the cytosol to the cell exterior, reduces cellular Mn levels, and protects against Mn toxicity (47). The efflux activity of SLC30A10 is specific to Mn (47–49). Using full body– and tissue-specific *Slc30a10* knockout mice, we identified two critical functions of SLC30A10 at the whole organism level—SLC30A10 localizes to the apical domain of hepatocytes and enterocytes to mediate hepatic and intestinal Mn excretion, and, additionally, SLC30A10 is active in the brain, where it mediates neuronal Mn efflux to provide additional neuroprotection (50, 51) [note that ~80% of the body burden of Mn is excreted by the liver, and the intestines excrete the remaining ~20% (10, 33)]. The role of SLC30A10 in Mn excretion was subsequently also confirmed by another group (52). Thus, Mn

neurotoxicity upon loss-of-function of SLC30A10 is a consequence of blocked Mn excretion and an inhibition of neuronal Mn efflux (reviewed in refs. 11 and 53). Similar studies on SLC39A14 by several groups identified it to be a Mn influx transporter that, at the organism level, is essential for the transport of Mn from blood into the liver and intestines for subsequent excretion by SLC30A10 (50, 54–59). Thus, the loss of function of SLC39A14 also induces Mn neurotoxicity by blocking Mn excretion (reviewed in refs. 11 and 53). Other work identified SLC39A8 to be a hepatic Mn importer that reclaims Mn excreted into bile to prevent Mn deficiency (60). Unlike SLC30A10, SLC39A14 and SLC39A8 also transport other divalent metals in vitro (61), but their primary in vivo function under physiological conditions appears to be Mn transport. Put together, the recent studies described above establish SLC30A10, SLC39A14, and SLC39A8 as essential human Mn transporters.

Based on the identification of SLC30A10, SLC39A14, and SLC39A8 as indispensable Mn transporters, we hypothesized that Mn homeostasis may be regulated by changes in these transporters. Here, we test this hypothesis and define the up-regulation of SLC30A10 in the liver and intestines to be a fundamental homeostatic response to elevated Mn that protects against Mn toxicity. The underlying mechanism is the activation of hypoxia-inducible factor (HIF) 1 and HIF2 due to an inhibitory effect of elevated levels of Mn on the prolyl hydroxylation and subsequent degradation of HIF proteins. We further show that small molecule inhibitors of prolyl hydroxylase enzymes, which stabilize HIF proteins, protect cells and mice against Mn toxicity. In totality, our studies identify a central regulatory pathway for the homeostatic control of Mn in mammals that may be leveraged for the management of Mn neurotoxicity in humans.

Results

Mn Exposure Up-Regulates SLC30A10 in the Mouse Liver or Intestine.
To test the hypothesis that Mn homeostasis may be regulated by changes in critical Mn transporters, we exposed mice to a daily drinking water–based Mn exposure regimen that models environmental Mn exposure in humans (11). In consideration of strain-specific effects, we performed this experiment in congenic 129S4/SvJaeJ or C57BL/6J mice, which are widely used in biomedical research. Epidemiological studies indicate that neurotoxicity from environmental Mn exposure primarily affects human children and adolescents (14–24). To recapitulate exposure across these developmentally sensitive early life periods, we dosed mice with Mn from birth until 8 wk of age when they attain adulthood (62) and assayed for changes in transporter expression using qRT-PCR. Mn treatment increased levels of SLC30A10 in the liver of
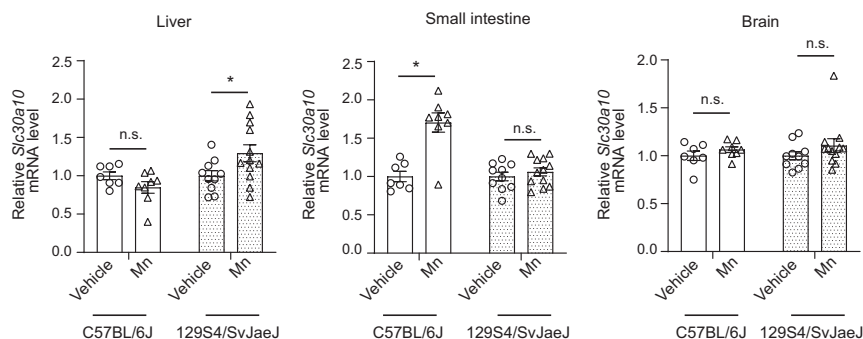

Fig. 1. Mn exposure increases SLC30A10 expression in the liver of 129S4/SvJaeJ and intestines of C57BL/6J mice. qRT-PCR analyses from indicated tissues of 129S4/SvJaeJ or C57BL/6J mice treated with vehicle or oral Mn (~15 mg absolute Mn/kg body weight daily) from PND1 until 8 wk of age. Animals were euthanized at 8 wk of age. For each strain, the mean expression in vehicle-treated mice was normalized to 1. n = 10 vehicle and 12 Mn for 129S4/SvJaeJ, and 7 vehicle and 8 Mn for C57BL/6J mice. Mean ± SE, *P < 0.05 by two-way ANOVA (strain and Mn treatment as independent variables) and Sidak's post hoc test for indicated comparisons; n.s., not significant.

Liu et al.
Up-regulation of the manganese transporter SLC30A10 by hypoxia-inducible factors
defines a homeostatic response to manganese toxicity

129S4/SvJaeJ but not C57BL/6J mice (Fig. 1). In contrast, there was a Mn-induced increase in SLC30A10 levels in the intestines of C57BL/6J but not 129S4/SvJaeJ mice (Fig. 1). The Mn regimen did not impact expression of SLC30A10 in the brain of either strain (Fig. 1). Hepatic and brain SLC39A14 and SLC39A8 levels were elevated in the 129S4/SvJaeJ strain, while intestinal SLC39A14 levels were enhanced in C57BL/6J mice (*SI Appendix*, Fig. S1 *A and B*). Intestinal SLC39A8 levels did not change in either strain (*SI Appendix*, Fig. S1*B*). We also observed modest strain- and organ-dependent changes in two other known Mn transporters—SPCA1, which transports Mn and Ca from the cytosol into the Golgi (63), and the divalent metal importer DMT1 (13)—as well as in the Fe efflux transporter Fpn (*SI Appendix*, Fig. S1 *C–E*). We drew two important conclusions from these animal studies: 1) the Mn-induced up-regulation of SLC30A10 and SLC39A14 in the digestive system may be homeostatically important, as it was detected in two strains of mice, albeit in different organs; and 2) strain-specific effects may make it challenging to interpret rodent studies of Mn homeostasis; instead, a comprehensive mechanistic understanding of the homeostatic control of Mn using disease-relevant culture models was necessary before well-controlled animal studies could be designed.

Mn Transcriptionally Up-Regulates SLC30A10. Based on the above, we utilized cell-based systems for subsequent studies. We used human-derived HepG2 hepatic cells for detailed assays because 1) the liver is the primary organ that excretes Mn, 2) a robust Mn-induced increase in hepatic SLC30A10 and SLC39A14 was detected in 129S4/SvJaeJ mice (Fig. 1 and *SI Appendix*, Fig. S1*A*), and 3) HepG2 cells express SLC30A10 and SLC39A14 and are amenable to genetic manipulation. Subsequently, we used primary human hepatocytes to validate key findings (see Fig. 9 later). In HepG2 cells, Mn treatment significantly elevated SLC30A10 but not SLC39A14 levels (*SI Appendix*, Table S1). Dose–response experiments revealed that SLC30A10 levels were elevated in cultures exposed to levels of Mn as low as 62.5 μM (Fig. 2*A*), which produced intracellular Mn levels equivalent to ~0.1 pg/cell (compared to ~1 fg/cell in vehicle-treated control cells) (Fig. 2*B*).

Time course assays showed that Mn rapidly up-regulated SLC30A10 with statistically significant increases evident within 2 h, and levels returned to baseline by 24 h (Fig. 2*C*). Immunoblot analyses confirmed that Mn increased SLC30A10 protein levels (Fig. 2*D*). Overall, these results 1) identify the up-regulation of SLC30A10 to be a primary response to elevated Mn exposure in hepatic systems in vitro, 2) indicate that SLC30A10 expression is highly sensitive to cellular Mn levels, with increases in Mn causing rapid elevations in SLC30A10, and 3) are consistent with the effects of Mn on SLC30A10 expression observed in preceding mouse studies.

SLC30A10 Is Transcriptionally Up-Regulated by Mn, and a Hypoxia Response Element in the SLC30A10 Promoter Is Required. We then focused on elucidating the mechanisms of the Mn-induced up-regulation of SLC30A10 (we did not further pursue effects of Mn on SLC39A14 because of the lack of an Mn-induced elevation in cell culture). Pretreatment with the transcription inhibitor actinomycin D (64) blocked the increase in SLC30A10 messenger RNA (mRNA) after Mn exposure in HepG2 cells (Fig. 3*A*), indicating that transcriptional activity was required for the SLC30A10 response and raising the hypothesis that *SLC30A10* gene expression may be transcriptionally up-regulated by elevated Mn. To test this, we first used a promoter–reporter approach. We fused the promoter of *SLC30A10* (nucleotides −679 to +211 relative to the start of transcription of *SLC30A10* gene) upstream of the luciferase gene (this construct is referred as SLC30A10$^{-679\ to\ +211}$luc) (Fig. 3*B*) and used lentivirus to generate HepG2 cells that stably expressed this construct. Treatment with Mn increased luciferase activity in cells expressing SLC30A10$^{-679\ to\ +211}$luc, while as expected, there was no change in cells expressing a luciferase-only control construct (Fig. 3 *B* and *C*). Thus, the promoter of *SLC30A10* contains a sequence element that responds to elevated Mn by increasing downstream gene transcription. To identify this sequence element, we deleted aspects of the promoter in SLC30A10$^{-679\ to\ +211}$luc (Fig. 3*B*), stably infected HepG2 cells with the generated constructs, and repeated the luciferase assay. The Mn-induced increase in luciferase activity was evident in cells
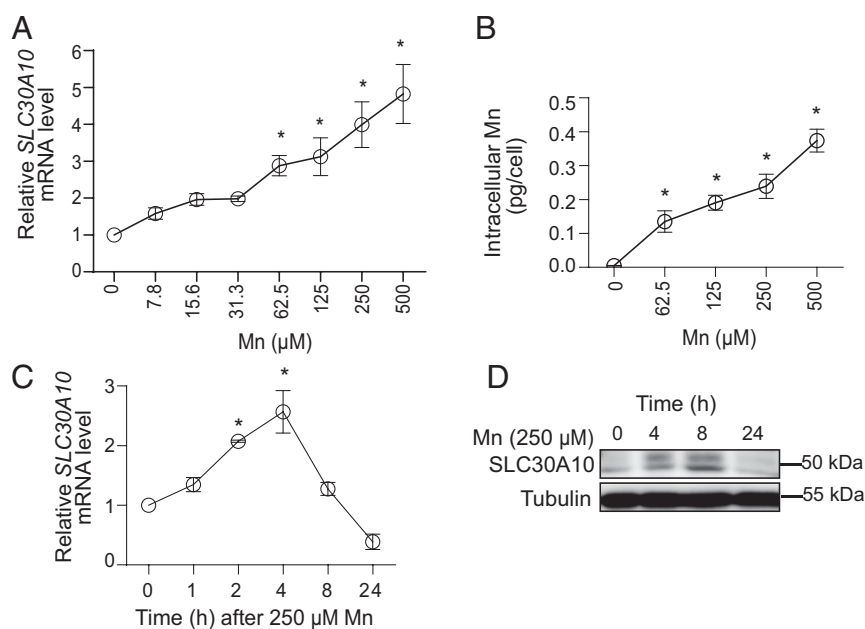

Fig. 2. Mn up-regulates SLC30A10 expression in HepG2 cells. (*A–C*) qRT-PCR analyses (*A* and *C*) or intracellular Mn levels (*B*). In *A* and *B*, Mn treatment was for 4 h at indicated concentrations. In *C*, Mn was used at 250 μM for indicated times. Expression without Mn treatment is normalized to 1 in *A* and *C*. n = 3 for *A* and *C*, and n = 4 for *B*. Mean ± SE, *$P < 0.05$ by one-way ANOVA and Dunnett's post hoc test for the comparison between no Mn and other conditions. (*D*) Immunoblot assays after treatment with 250 μM Mn for indicated times.
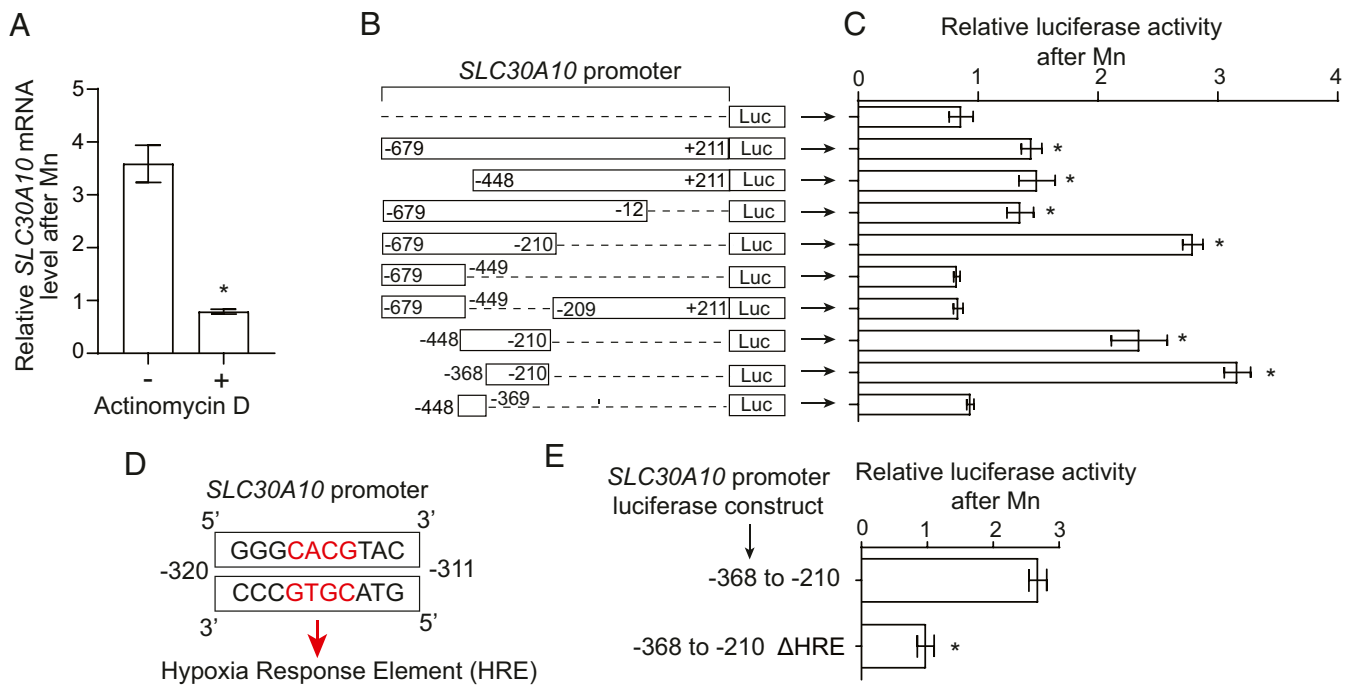
Liu et al.
Up-regulation of the manganese transporter SLC30A10 by hypoxia-inducible factors defines a homeostatic response to manganese toxicity

PNAS | 3 of 12
https://doi.org/10.1073/pnas.2107673118

Fig. 3. The Mn-induced up-regulation of SLC30A10 in HepG2 cells requires a hypoxia response element in the *SLC30A10* promoter. (*A*) qRT-PCR analyses after pretreatment of cells with vehicle DMSO or actinomycin D (5 μM) for 30 min followed by exposure to 0 or 250 μM Mn for 4 h. Expression without Mn treatment was normalized to 1 in DMSO- or actinomycin D–treated cells separately. $n = 3$. Mean ± SE, *$P < 0.05$ by Student's t test. (*B*–*E*) Schematic of luciferase (Luc) reporter constructs used (*B*), the required hypoxia response element (shown in red) in the *SLC30A10* promoter (*D*), and relative normalized luciferase signal after Mn treatment in cells expressing indicated luciferase constructs (*C* and *E*). In *B* and *D*, the numbers indicate the position relative to the start of transcription. The hypoxia response element (HRE) highlighted in red in *D* was deleted in the ΔHRE construct in *E*. For *C* and *E*, cells were treated with or without 250 μM Mn for 16 h. Luciferase signals were normalized to protein in each sample. For each construct, values after Mn treatment are expressed relative to that without Mn normalized to 1. $n \geq 3$. Mean ± SE, *$P < 0.05$ by one-way ANOVA and Dunnett's post hoc test for the comparison between luciferase only and other conditions in *C* and Student's t test in *E*.

expressing SLC30A10$^{-679 \text{ to } -12}$luc or SLC30A10$^{-679 \text{ to } -210}$luc but not SLC30A10$^{-679 \text{ to } -449}$luc (Fig. 3 *B* and *C*), suggesting that residues −448 to −210 contained the Mn-responsive element. Indeed, SLC30A10$^{\Delta-448 \text{ to } -210}$luc failed to respond to Mn, while SLC30A10$^{-448 \text{ to } -210}$luc exhibited a robust response (Fig. 3 *B* and *C*). Thus, residues −448 to −210 of the *SLC30A10* promoter are required and sufficient to mediate the Mn-induced increase in transcription. Through a subsequent set of deletion analyses, we refined the required and sufficient sequence to residues −368 to −210 in the *SLC30A10* promoter (Fig. 3 *B* and *C*). Bioinformatic analyses using the PROMO-ALGGEN algorithm (65, 66) revealed that the −368 to −210 region contained putative binding sites for C/EBPB, YY1, RXR-α, HIF, P53, and c-Jun transcription factors. The expression of dominant-negative versions of C/EBPB, YY1, RXR-α, P53, or c-Jun did not affect the Mn-induced up-regulation of SLC30A10 mRNA (*SI Appendix*, Fig. S2*A*). As a positive control, we verified that the dominant-negative mutants produced expected changes in the expression of their known target genes (67–71)—an increase in MAP1LC3B, CDKN1A, or CYP7A1 mRNA with dominant-negative c-Jun, C/EBPB, or RXR-α, respectively, and a decrease in CDK6 or PUMA mRNA with dominant-negative YY1 or P53, respectively (*SI Appendix*, Fig. S2*B*). Thus, the Mn-induced up-regulation of SLC30A10 is independent of C/EBPB, YY1, RXR-α, P53, and c-Jun. We could not use a dominant-negative approach to inhibit HIF (see knockdown studies in the next section). Instead, we deleted the only hypoxia response element within the −368 to −210 region of the *SLC30A10* promoter [5′RCGTG (72)], which is the binding site for HIF transcription factors (Fig. 3*D*), and repeated the luciferase assay. Importantly, the deletion of this hypoxia response element abolished the Mn-induced increase in

luciferase activity (Fig. 3*E*). In totality, Mn transcriptionally up-regulates SLC30A10, and a hypoxia response element in the promoter of *SLC30A10* is required.

Transcriptional Activity of HIF1 or HIF2 Is Required and Sufficient to Increase SLC30A10 Expression after Mn Exposure. The above results suggested that HIF transcription factors likely mediate the Mn-induced up-regulation of SLC30A10. HIFs are heterodimeric transcription factors formed by the association of an α subunit, the most well studied of which are HIF1-α or HIF2-α, with a common β subunit (HIF1-β/ARNT) (72). The transcriptionally active moieties are named after the α subunits. Both HIF1 and HIF2 bind the canonical hypoxia response element (73). Under normoxic conditions, HIF-α subunits are rapidly hydroxylated by prolyl hydroxylases, subsequently bound by the von Hippel–Lindau (VHL) protein complex, ubiquitinated, and targeted for proteasomal degradation (72, 74). Hypoxia inhibits prolyl hydroxylases, leading to an increase in HIF1-α or HIF2-α protein levels and allowing for the formation of transcriptionally active heterodimeric complexes with HIF1-β/ARNT (72, 74). Notably, elevated levels of divalent metals also inhibit prolyl hydroxylases, which are Fe-containing enzymes, and increase HIF1-α protein levels as well as HIF1-dependent transcription (75–81). The precedent for the hypoxia-mimetic effect of metals provided further support for the hypothesis that elevated Mn may induce SLC30A10 expression by activating HIFs. However, before directly testing this hypothesis, it was essential to confirm that HIFs were indeed activated in our experimental system. We observed that treatment with Mn increased protein levels of HIF1-α and HIF2-α in HepG2 cells (Fig. 4 *A*–*C*). The increase was evident at 4 h and returned to baseline by 24 h (Fig. 4 *A*–*C*),

similar to the time course of the SLC30A10 response (Fig. 2). Furthermore, HIF1-α and HIF2-α were detected in the nucleus of Mn-treated cells (Fig. 4D), which is necessary for transcriptional activity. Finally, Mn also enhanced expression of *VEGF* (*SI Appendix*, Table S1), a canonical HIF1 target gene (72). These findings indicated that Mn treatment activated HIF transcription factors and, combined with the luciferase reporter assays, provided strong justification to test for the requirement of HIF1 or HIF2 for the Mn-induced SLC30A10 response.

To test for the role of HIF1 or HIF2, we used a lentivirus-based short hairpin RNA (shRNA) system to stably knockdown HIF1-α or HIF2-α in cells. Both shRNAs significantly depleted the targeted gene product (*SI Appendix*, Table S2); a compensatory increase in HIF1-α mRNA was detected with HIF2-α knockdown (*SI Appendix*, Table S2). However, despite efficient knockdown, the Mn-induced elevation of VEGF or SLC30A10 was only modestly attenuated (Fig. 5 A and B). The lack of a strong inhibitory effect of knockdown of either gene product could be due to redundancy. To test this, we depleted the common HIF1-β/ARNT subunit using two separate shRNAs. Each shRNA had a knockdown efficiency of ~50% (*SI Appendix*, Table S2), and each shRNA partially inhibited the Mn-induced elevation of VEGF and SLC30A10 by ~50 to 60% relative to scramble (Fig. 5C). The failure of HIF1-β/ARNT knockdown to also completely abolish the SLC30A10 response could be a consequence of incomplete knockdown or indicate that another transcription factor was involved. Therefore, in subsequent experiments, we generated HIF1-α and HIF2-α double-knockdown cells by performing sequential lentiviral infections. The knockdown efficiency of HIF1-α was ~80% and of HIF2-α was ~65% (*SI Appendix*, Table S2). Notably, the ability of Mn to enhance SLC30A10 expression was very strongly repressed in the double-knockdown cells, and relative to scramble shRNA, the Mn-induced increase of SLC30A10 was inhibited by ~90% in the double-knockdown cells (Fig. 5D). A similar strong inhibition of the Mn-induced elevation of VEGF was also observed (Fig. 5D). For further validation, we used the small molecule LW6, which degrades HIF-α subunits by inducing expression of VHL (82). Importantly, LW6 treatment robustly blocked the Mn-induced up-regulation of SLC30A10 and VEGF (Fig. 5E), and furthermore, LW6 also abolished the Mn-induced increase in the activity of the SLC30A10 promoter luciferase reporter (Fig. 5F). Put together, data from the knockdown and LW6 assays indicate that activity of HIF1 or HIF2 is obligatorily required for the Mn-induced up-regulation of SLC30A10. Finally, the expression of VHL-insensitive versions of mouse HIF1-α or HIF2-α that could not get prolyl hydroxylated and were therefore expressed at high levels under normoxic conditions increased SLC30A10 levels independent of Mn exposure (Fig. 5G), implying that the activity of either HIF1 or HIF2 is sufficient to up-regulate SLC30A10. Overall, our results indicate that the Mn-induced transcriptional up-regulation of SLC30A10 is mediated by HIF1 and HIF2 in a redundant manner.

Mn Inhibits the Prolyl Hydroxylation of HIF-α Subunit. To elucidate the mechanism by which Mn increased HIF-α protein levels, we assayed for changes in HIF1-α prolyl hydroxylation in HepG2 cells because 1) metals are known inhibitors of the prolyl hydroxylation of HIF-α subunits (77–80); 2) although Mn increased HIF1-α or HIF2-α protein levels by 4 h (Fig. 4A), levels of HIF1-α or HIF2-α mRNA were not elevated at this time point (Fig. 6A), suggesting that the increase in HIF1-α and HIF2-α protein was posttranslational; and 3) a specific and sensitive antibody against human hydroxyprolyl HIF1-α was available. Since prolyl hydroxylated HIF1-α is rapidly degraded in the proteasome (72, 74), the assay was performed with or without treatment with the proteasome inhibitor MG132. In the absence of MG132, prolyl hydroxylated HIF1-α was not detected irrespective of Mn treatment (Fig. 6B), but similar to results in Fig. 4A, total HIF1-α levels were elevated after Mn treatment (Fig. 6B). Proteasome inhibition led to the accumulation of prolyl hydroxylated HIF1-α in cells that had not been exposed to Mn (Fig. 6B). Importantly, however, signals for prolyl hydroxylated HIF1-α were substantially lower in the Mn-treated condition, and total HIF1-α levels of Mn-treated cells were greater than in those not treated with Mn (Fig. 6B). Finally, levels of prolyl hydroxylase domain 2 (PHD2), the primary enzyme that hydroxylates HIF-α subunits (74), were elevated in Mn-treated cells (Fig. 6A), ruling out the possibility that the observed reduction in prolyl hydroxylation of HIF1-α was a consequence of a decrease in prolyl hydroxylase gene expression. Thus, Mn inhibits prolyl hydroxylation of HIF-α subunits, which increases HIF-α protein levels and induces HIF-dependent transcription.
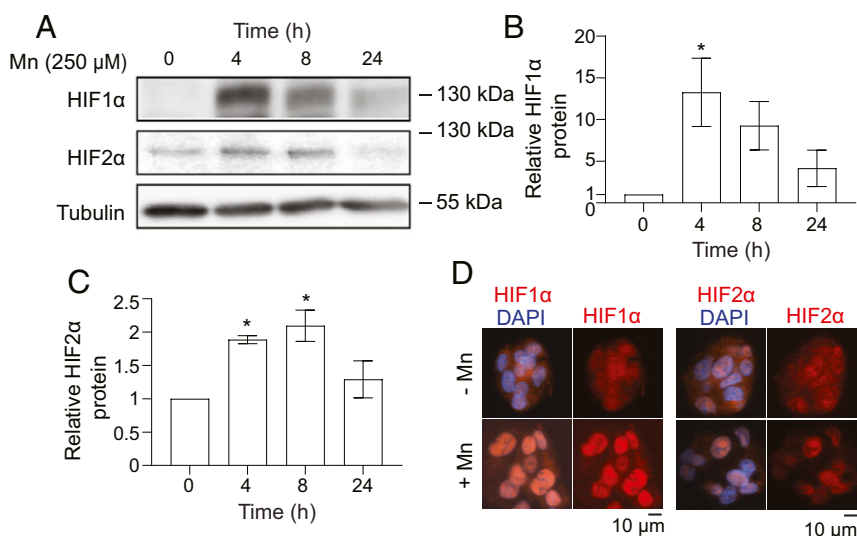

Fig. 4. Mn stabilizes and induces nuclear accumulation of HIF1-α and HIF2-α protein in HepG2 cells. (A) Immunoblot analyses after treatment with 0 or 250 μM Mn for indicated times. (B and C) Quantification of HIF1-α or HIF2-α levels normalized to tubulin from A. n = 3. Mean ± SE, *P < 0.05 by one-way ANOVA and Dunnett's post hoc test for comparisons between 0 h and other groups. (D) Immunofluorescence after treatment with or without 250 μM Mn for 4 h.
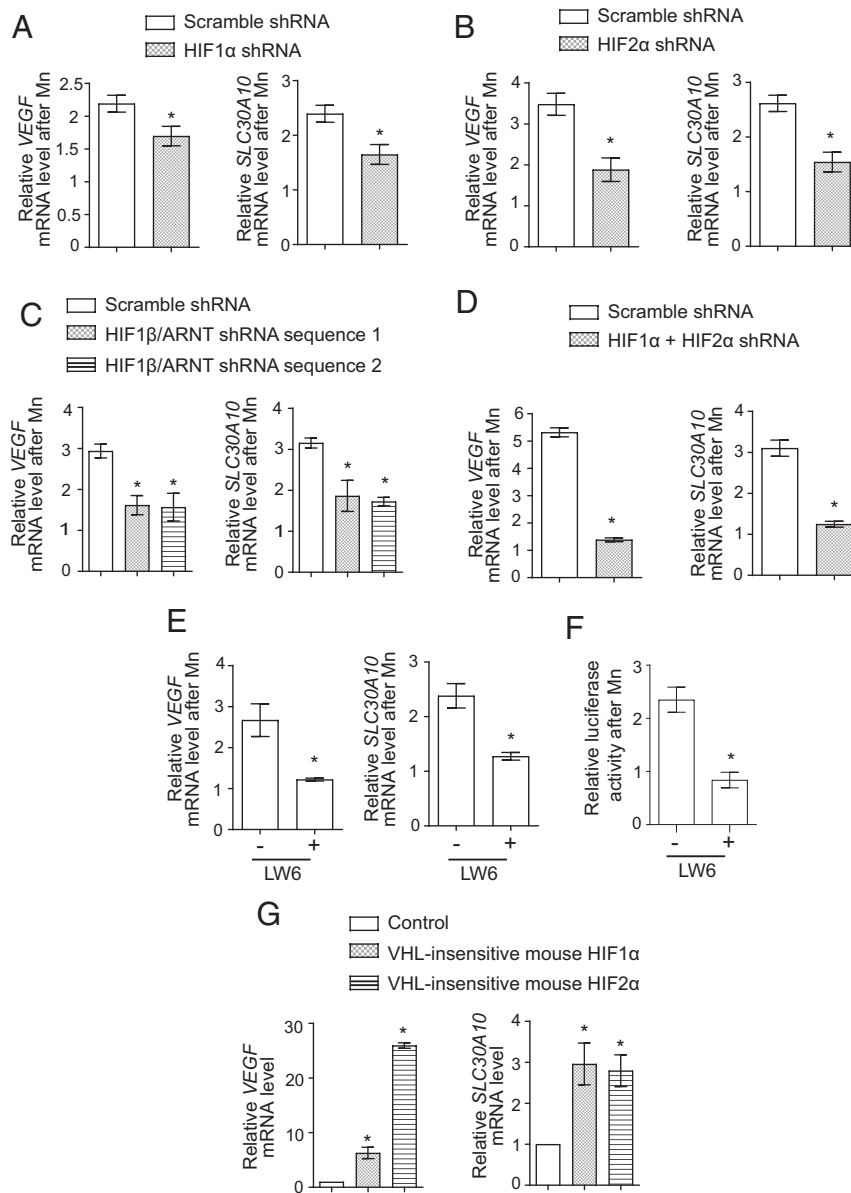
Fig. 5. HIF1 or HIF2 are required and sufficient for the Mn-induced up-regulation of SLC30A10 expression. (*A*–*D*) qRT-PCR analyses in HepG2 cells stably expressing shRNAs with a scrambled sequence or targeting HIF1-α (*A*), HIF2-α (*B*), HIF1-β/ARNT (*C*), or HIF1-α and HIF2-α (*D*) and treated with or without 250 μM Mn for 4 h. Scramble shRNA sequence 1 was used for experiments with HIF1-α shRNA (*A*) while scramble shRNA sequence 2 was used for the other experiments (*B–D*). For each infection condition, expression without Mn was normalized to 1. $n = 3$ to 4. Mean ± SE, *$P < 0.05$ by Student's *t* test (*A, B,* and *D*) or one-way ANOVA and Dunnett's post hoc test for the comparison between scramble shRNA and other groups (*C*). (*E*) qRT-PCR in HepG2 cells treated with or without 10 μM LW6 for 1 h followed by exposure to 0 or 250 μM Mn for 4 h. For cells that did or did not receive LW6, expression without Mn was separately normalized to 1. $n = 5$. Mean ± SE, *$P < 0.05$ by Student's *t* test. (*F*) Relative normalized luciferase activity in cells stably expressing SLC30A10$^{-368 \text{ to } -210}$luc after treatment with or without 10 μM LW6 for 1 h followed by 0 or 250 μM Mn for 16 h. For cells that did or did not receive LW6, separately, luciferase activity was measured with or without Mn treatment, normalized to protein concentration, and the value for the group without Mn treatment was expressed as 1. $n = 3$. Mean ± SE, *$P < 0.05$ by Student's *t* test. (*G*) qRT-PCR analyses in control HepG2 cells or cells stably expressing VHL-insensitive mouse HIF1-α or HIF2-α. Expression in control-infected cells was normalized to 1. $n = 3$. Mean ± SE, *$P < 0.05$ by one-way ANOVA and Dunnett's post hoc test for comparisons between control and other groups.

The Mn-Induced Up-Regulation of SLC30A10 Is a Critical, Homeostatic Protective Response. To determine the physiological relevance of the Mn-induced increase in SLC30A10, we compared intracellular metal levels and the viability of HIF1-β/ARNT knockdown HepG2 cells, in which the SLC30A10 response is inhibited, with controls. As both HIF1-β/ARNT shRNAs were equally effective in inhibiting the SLC30A10 response (Fig. 5*C*), the metal measurement and viability assays were performed using only one shRNA. Under basal conditions, Mn levels of the knockdown cells were comparable to scramble shRNA-infected control (Fig. 7*A*). However, after Mn treatment, Mn levels in HIF1-β/ARNT knockdown cells were higher than controls (Fig. 7*A*). Levels of other metals (Fe, Cu, and Zn) were unaltered (*SI Appendix*, Fig. S3). Furthermore, HIF1-β/ARNT knockdown cells were more sensitive to Mn-induced death (Fig. 7*B*). These results suggest that the up-regulation of SLC30A10 is a critical homeostatic response to elevated Mn exposure that reduces intracellular Mn levels and protects against Mn toxicity.
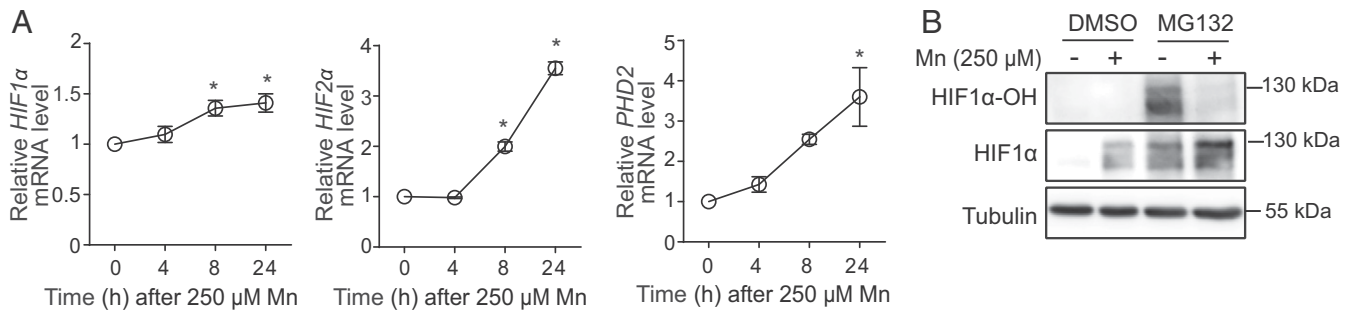
Fig. 6. Mn inhibits the prolyl hydroxylation of HIF1-α. (*A*) qRT-PCR analyses in HepG2 cells treated with 250 μM Mn for indicated times. Expression in cells that did not receive Mn was normalized to 1. *n* = 3. Mean ± SE, **P* < 0.05 by one-way ANOVA and Dunnett's post hoc test for comparison between no Mn and other groups. (*B*) Immunoblot analyses of whole-cell lysates obtained from HepG2 cells treated with or without 10 μM MG132 for 1 h followed by exposure to 0 or 250 μM Mn for 4 h. HIF1-α–OH, prolyl hydroxylated HIF1-α.

Prolyl Hydroxylase Inhibitors Protect Cells against Mn Toxicity. Roxadustat, vadadustat, and molidustat are small molecule inhibitors of prolyl hydroxylases that have completed, or are in, advanced clinical trials for the treatment of renal anemia (83–86). By inhibiting prolyl hydroxylase enzymes, these compounds increase HIF-α protein and activate HIF-dependent transcription (83–86). Our discovery that SLC30A10 is up-regulated by HIF1/HIF2 raised the hypothesis that prolyl hydroxylase inhibitors may induce SLC30A10 expression, reduce Mn levels, and protect against Mn toxicity. In HepG2 cells, roxadustat or vadadustat increased levels of HIF1-α and HIF2-α protein (Fig. 8*A*) and enhanced expression of SLC30A10 in a concentration- and time-dependent manner (Fig. 8 *B* and *C*). Furthermore, while roxadustat or vadadustat did not impact intracellular Mn in cells not exposed to Mn, under conditions of elevated Mn exposure, intracellular Mn levels of cells treated with roxadustat or vadadustat were significantly lower than controls (Fig. 8*D*). The levels of other metals (Fe, Cu, and Zn) were not altered by drug treatment (*SI Appendix*, Fig. S4), indicating that the effect was specific to Mn. Roxadustat or vadadustat also protected cells against Mn-induced cell death (Fig. 8*E*). Similar results were obtained with molidustat (*SI Appendix*, Fig. S5 *A–C*). Thus, prolyl hydroxylase inhibitors increase SLC30A10 expression, reduce intracellular Mn levels, and protect cells against Mn toxicity.

Validation of Results in Primary Human Hepatocytes. To validate the physiological relevance of results obtained in HepG2 cells, we performed confirmatory assays in primary human hepatocytes. Importantly, in the primary system, treatment with Mn increased VEGF or SLC30A10 expression, and this increase was inhibited by the HIF inhibitor LW6 (Fig. 9*A*). Additionally, treatment with roxadustat or vadadustat also increased VEGF or SLC30A10 expression (Fig. 9*B*). These results validate the primary conclusions of findings from HepG2 cells and indicate that Mn increases SLC30A10 expression in a HIF-dependent manner in primary hepatocytes.

Roxadustat Protects Mice against Mn Neurotoxicity. Based on the compelling cell culture data, we expanded our analyses to mice and performed a proof-of-principle protection experiment using roxadustat. We used C57BL/6J mice for this assay because 1) neurobehavioral outcomes are well characterized in this strain, 2) we observed that roxadustat treatment increased intestinal SLC30A10 levels in these animals (Fig. 10*A*), and 3) similar to an increase in hepatic SLC30A10, increased intestinal SLC30A10 is expected to enhance Mn excretion. We assayed for neurological function using the open-field test. The first 5-min interval of the test provides information about behavioral reactivity and exploratory behavior of rodents in a novel environment and increases in activity in this interval may be indicative of anxiety-like

disorders. The succeeding 10-min interval is a measure of the generalized locomotor activity of the animals and decreases in this interval are indicative of neuromotor deficits. There were no differences between groups in the first 5-min interval (Fig. 10*B*). In the 6- to 15-min interval, consistent with a neuromotor dysfunction, animals exposed to Mn only exhibited reduced vertical (i.e., rearing) movement than vehicle-treated controls (Fig. 10*B*). Importantly, this hypolocomotor phenotype was not detected in mice treated with Mn and roxadustat (Fig. 10*B*), and additionally, roxadustat treatment by itself did not impact activity (Fig. 10*B*). Tissue metal measurements performed after the completion of the neurobehavioral test revealed that, as expected, there was a main effect of Mn treatment in increasing brain Mn levels (Fig. 10*C*), and a trend toward an increase in blood Mn was also evident (Fig. 10*C*). Notably, there was a main effect of roxadustat in reducing brain Mn levels (Fig. 10*C*), providing an explanation for the neuroprotective effect of roxadustat in the open-field test. Changes in Mn were specific because levels of other metals (Fe, Cu, and Zn) were not impacted by Mn exposure or roxadustat treatment (*SI Appendix*, Fig. S6). Roxadustat did not
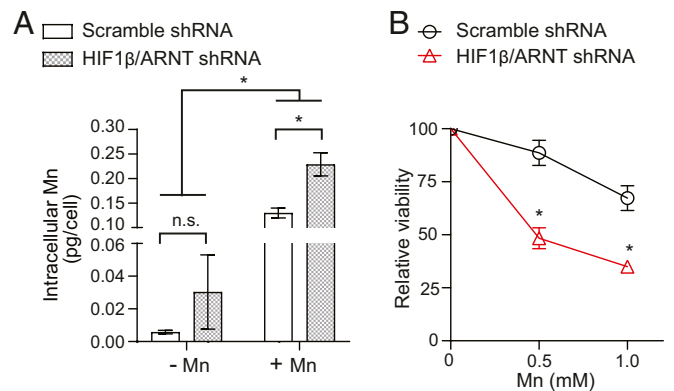

Fig. 7. The activation of HIF transcription factors by Mn is a homeostatic protective response against Mn toxicity. (*A*) Inductively coupled plasma mass spectrometry analyses to measure intracellular metal levels in HepG2 cells stably infected with scramble shRNA (sequence 2) or HIF1-β/ARNT shRNA (sequence 1) and treated with or without 125 μM Mn for 16 h. *n* = 3. Mean ± SE, **P* < 0.05 by two-way ANOVA (shRNA and Mn treatment as independent variables) and Sidak's post hoc test for indicated comparisons; n.s., not significant. (*B*) Cell viability assays in scramble (sequence 2) or HIF1-β/ARNT shRNA (sequence 1)-infected HepG2 cells treated with 0, 0.5, or 1 mM Mn for 16 h. Viability of scramble or ARNT shRNA-infected cells that did not receive Mn was separately normalized to 100. *n* = 3. Mean ± SE, **P* < 0.05 by two-way ANOVA (shRNA and Mn treatment as independent variables) and Sidak's post hoc test for comparisons between infection conditions at each Mn dose.
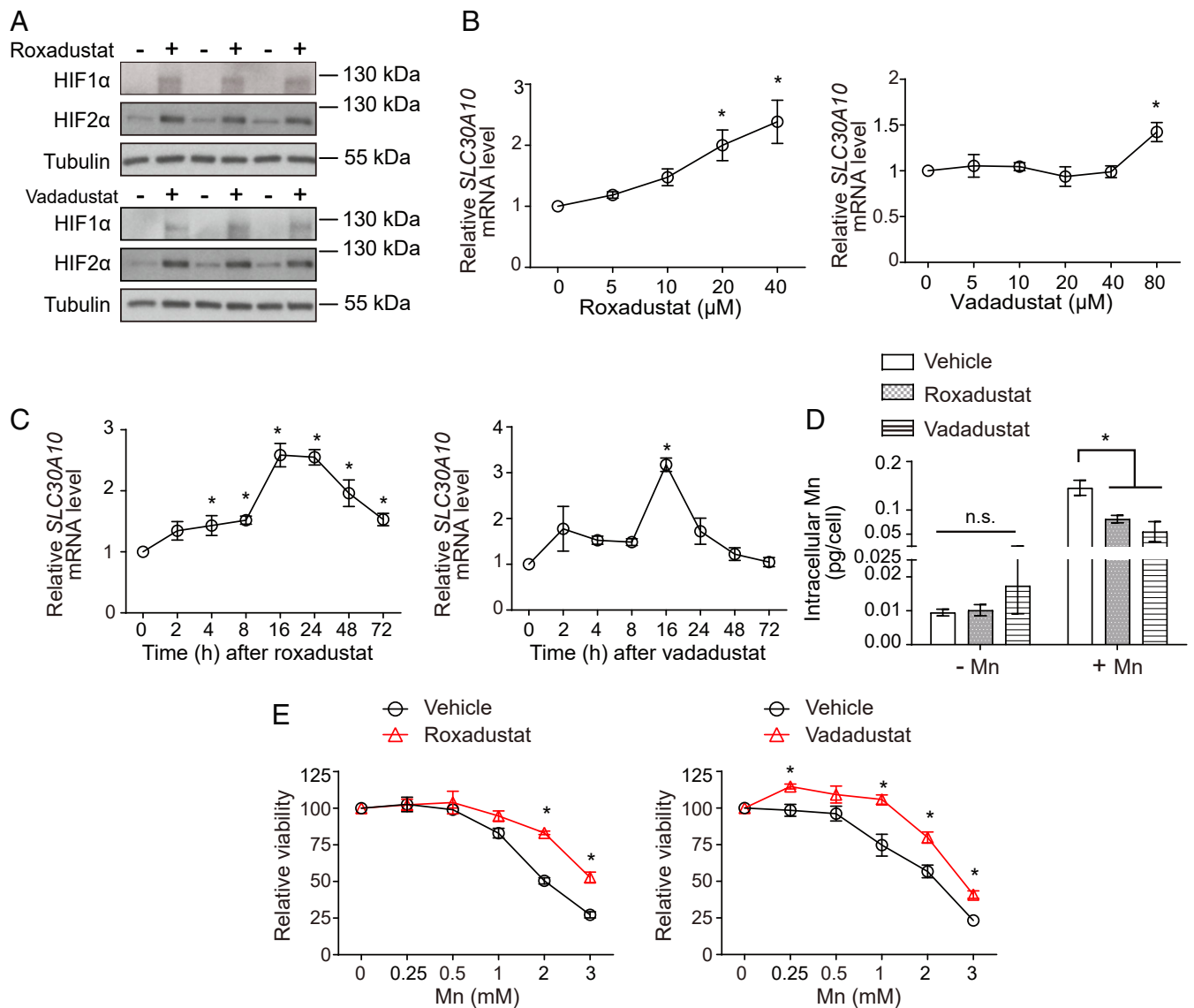
Liu et al.
Up-regulation of the manganese transporter SLC30A10 by hypoxia-inducible factors defines a homeostatic response to manganese toxicity

PNAS | 7 of 12
https://doi.org/10.1073/pnas.2107673118

Fig. 8. Prolyl hydroxylase inhibitors enhance SLC30A10 levels, reduce intracellular Mn, and protect HepG2 cells against Mn toxicity. (*A*) Immunoblot assays in cells treated with or without 20 μM roxadustat or 80 μM vadadustat for 16 h. (*B* and *C*). qRT-PCR after treatment with indicated doses of roxadustat or vadadustat for 16 h (*B*) or 20 μM roxadustat or 80 μM vadadustat for indicated times (*C*). Expression in cells that did not receive the drug was normalized to 1. $n \geq 3$. Mean ± SE, *$P < 0.05$ by one-way ANOVA and Dunnett's post hoc test for comparison between no drug and other conditions. (*D*) Intracellular Mn levels in cells treated with or without 20 μM roxadustat or 80 μM vadadustat for 16 h followed by exposure to 0 or 125 μM Mn for 24 h. $n = 5$ to 6. Mean ± SE, *$P < 0.05$ by two-way ANOVA (drug and Mn treatment as independent variables) and Tukey Kramer post hoc test for indicated comparisons; n.s., not significant. (*E*) Cell viability assays after treatment with or without 20 μM roxadustat or 80 μM vadadustat for 16 h followed by exposure to indicated levels of Mn for 24 h. Viability of cells treated with or without prolyl hydroxylase inhibitors in the absence of Mn exposure were separately normalized to 100. $n = 3$. Mean ± SE, *$P < 0.05$ by two-way ANOVA (drug and Mn treatment as independent variables) and Sidak's post hoc test for comparisons between treatment conditions at each Mn dose.

impact brain SLC30A10 levels (Fig. 10*A*), suggesting that the protective effect of roxadustat against Mn neurotoxicity was unlikely to be a consequence of a direct reduction of brain Mn levels by elevations in SLC30A10 and instead more likely to be reflective of an increase in Mn excretion. Overall, roxadustat reduces brain Mn levels and protects against Mn neurotoxicity, suggesting that it may be useful for the treatment of neurological disease induced by Mn in humans.

Discussion

Prior knowledge about homeostatic responses to Mn in mammals was primarily derived from radiotracer Mn elimination and distribution assays performed in rodents in the 1950s to 60s. A

particularly important finding was that increased oral delivery of Mn by dietary supplementation enhanced the excretion of parenterally injected radioactive Mn (8–10). This and other related results suggested that body Mn levels are primarily controlled by changes in Mn excretion, with excretion increasing upon elevated Mn exposure (8–10). However, the molecular mechanisms were unclear, largely because transporters that control Mn levels in humans had not been identified until recently. Our current findings characterize the up-regulation of the Mn efflux transporter SLC30A10, which mediates Mn excretion (11, 47, 50, 51), in the liver and intestines to be a central protective response to elevated Mn exposure. The Mn-induced up-regulation of SLC30A10 provides a pathway to enhance Mn excretion and reduce Mn levels
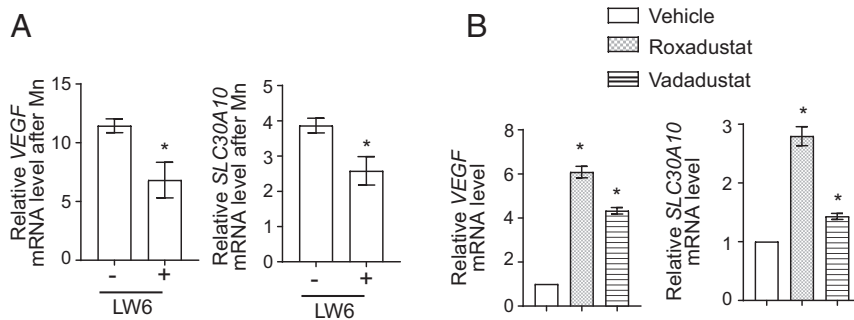
Liu et al.
Up-regulation of the manganese transporter SLC30A10 by hypoxia-inducible factors
defines a homeostatic response to manganese toxicity

Fig. 9. Mn treatment up-regulates SLC30A10 in a HIF-dependent manner in primary human hepatocytes. (*A* and *B*) qRT-PCR assays in cells treated with or without 10 μM LW6 for 1 h followed by 0 or 250 μM Mn for 4 h (*A*) or with or without 20 μM roxadustat or 80 μM vadadustat for 16 h (*B*). For *A*, separately for cells that did or did not receive LW6, expression in the absence of Mn treatment was normalized to 1. For *B*, expression in the absence of drug treatment was normalized to 1. *n* = 3. Mean ± SE, *P < 0.05 by Student's *t* test (*A*) or one-way ANOVA and Dunnett's post hoc test for the comparison between no drug and other conditions (*B*).

during Mn toxicity. These results are consistent with, and establish a molecular framework to contextualize, the historic radiotracer Mn elimination studies.

In humans, elevated exposure to Mn primarily occurs via inhalation in occupational settings or orally via drinking water because of environmental contamination (11). The oral Mn exposure regimen we utilized modeled human environmental Mn exposure (11). This regimen elevated SLC30A10 levels in the liver of 129S4/SvJaeJ and intestines of C57BL/6J mice but not the brain of either strain. The lack of an effect in the brain in our studies may be a consequence of the physiology of Mn absorption and

excretion with the liver/intestines, but not the brain, experiencing repeated Mn fluxes because of enterohepatic circulation. Additionally, there are striking genetic differences between congenic mouse strains (87, 88), and strain background is a well-established modulator of phenotypic outcomes (89, 90). As an example relevant to metal homeostasis, strain background strongly influences the severity of Fe accumulation in the *Hfe* knockout mouse model of hereditary hemochromatosis (91). Our results imply that genetic background also needs to be carefully considered when mouse studies of Mn homeostasis and neurotoxicity are designed. While determining the genomic basis of phenotypic divergence in
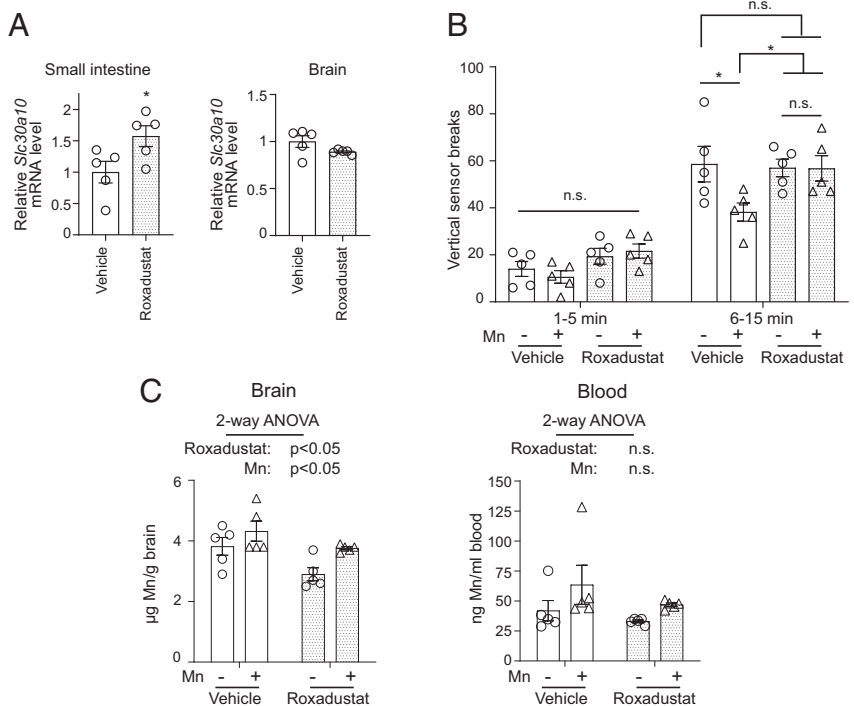
Fig. 10. Roxadustat protects mice against Mn neurotoxicity. (*A*) qRT-PCR assays from indicated tissues of C57BL/6J mice harvested after treatment with vehicle or roxadustat (10 mg/kg body weight daily intraperitoneally) for 4 wk (starting at ~4 wk of age). Mean expression in vehicle-treated mice was normalized to 1. *n* = 5/treatment. Mean ± SE, *P < 0.05 by Student's *t* test. (*B*) Open-field activity data for vertical movement in mice treated with vehicle or roxadustat as described in *A* along with or without exposure to Mn in drinking water (~30 mg absolute Mn/kg body weight daily). Treatment was at ages and for the duration described in *A*. Open-field analysis was performed before euthanasia. *n* = 5/group. Mean ± SE, *P < 0.05 by repeated measures two-way ANOVA and Tukey Kramer post hoc test for indicated comparisons. (*C*) Inductively coupled plasma mass spectrometry metal analyses from indicated tissues of animals used for neurobehavior analyses in *B*. *n* = 5/group. Mean ± SE. Indicated *P* values are for two-way ANOVA analyses using roxadustat and Mn as independent variables; n.s., not significant.

Liu et al.
Up-regulation of the manganese transporter SLC30A10 by hypoxia-inducible factors
defines a homeostatic response to manganese toxicity

PNAS | 9 of 12
https://doi.org/10.1073/pnas.2107673118

congenic mouse strains is daunting, the emergence of such information for our findings in the future may provide insights into the homeostatic control and toxicity mechanisms of Mn.

Mn increased SLC30A10 expression by stabilizing HIF1-α and HIF2-α protein and activating HIF1/HIF2-dependent transcription. The underlying mechanism was an Mn-induced block in the prolyl hydroxylation of HIF-α subunits. As expression of the major human prolyl hydroxylase enzyme, PHD2, was not attenuated by Mn, it is likely that Mn inhibited the enzymatic activity of prolyl hydroxylase enzymes. This hypothesis is consistent with the known inhibitory effect of divalent metals on prolyl hydroxylases in other model systems (76–81). Prolyl hydroxylases are Fe-containing enzymes that utilize α-ketoglutarate as a cosubstrate and ascorbate as a cofactor (72, 74, 75). Mn may inhibit enzyme activity by direct binding (either replacing the required Fe or binding at another site) and/or indirectly altering cellular Fe, ascorbate, or α-ketoglutarate levels. Investigating whether Mn induces any of these possible effects in disease-relevant hepatic/intestinal systems and under Mn treatment conditions that model human exposure is an important next step.

The discovery that Mn activates HIF1/HIF2 to up-regulate SLC30A10 raises a few other important issues. First, the activation of HIF1/HIF2-mediated transcription may be an integral component of the homeostatic control of Mn as well as the pathobiology of Mn neurotoxicity in humans exposed to Mn. Suggestive evidence of HIF activation in patients with hereditary Mn neurotoxicity because of *SLC30A10* mutations already exists. These patients exhibit polycythemia, which is likely secondary to observed elevations in erythropoietin expression (37), and erythropoietin expression is regulated by HIF1 and induced by hypoxia or Mn (92). Second, determining whether HIF1 and HIF2 are truly redundant in mediating the SLC30A10 response at the organism level or whether the requirement of these factors depends on life stage, nature of Mn exposure, or cell type is critical. Third, recent epidemiological studies identified widely prevalent single nucleotide polymorphisms (SNPs) in *SLC30A10* associated with tissue Mn levels and neurological function in the general population (93, 94). Detailed analyses are necessary to determine whether previously studied or as yet uncharacterized SNPs in *SLC30A10* or *HIF* genes modulate the Mn-induced up-regulation of SLC30A10 in a manner that impacts the risks and outcomes of Mn neurotoxicity. Finally, vitamin D3 and bile acids were recently reported to induce expression of SLC30A10 in the intestines (95–97). Intestinal Mn excretion requires SLC30A10, and available evidence suggests that the role of the intestines in regulating systemic Mn levels gains prominence when the excretion of Mn by the liver is compromised or saturated (10, 33, 51). Therefore, studying the crosstalk between Mn/HIF, vitamin D3, and bile acid–mediated regulation of SLC30A10, especially under conditions of elevated Mn exposure, is essential to obtain a comprehensive understanding of Mn homeostasis at the organism level.

Definitive treatments are not available for Mn neurotoxicity. Bringing a new drug into clinical use is challenging, and the likelihood of success is higher if an existing drug can be repurposed. We discovered that prolyl hydroxylase inhibitors increase SLC30A10 levels and protect cells and mice against Mn toxicity. These molecules activate HIF-dependent transcription by stabilizing HIF-α subunits; are in, or have completed, advanced clinical trials for renal anemia; and one compound, roxadustat, is already approved for human use in China (83–86). Notably, our work indicates that prolyl hydroxylase inhibitors protect against Mn neurotoxicity by increasing Mn excretion. An inherent implication is that these drugs will not need to cross the blood–brain barrier for efficacy, which substantially enhances the possibility of therapeutic effectiveness. Thus, our findings identify prolyl hydroxylase inhibitors as promising pharmacological candidates for the management of Mn neurotoxicity.

Methods

Experimental procedures are described in detail in *SI Appendix* and briefly summarized below.

Animal Experiments. All animal experiments were approved by the Institutional Animal Care and Use Committee of the University of Texas at Austin. We used a well-established drinking water–based Mn exposure regimen that models human environmental Mn exposure (reviewed in our ref. 11). A detailed explanation of the justification of using this regimen to model human Mn exposure is provided in *SI Appendix*. Mice received ~50 mg $MnCl_2.4H_2O$/kg body weight daily (~15 mg absolute Mn/kg per day) from birth until 8 wk of age. For preweaning exposure, Mn was delivered by pipette directly into the mouth, and after weaning, Mn was delivered in drinking water. See *SI Appendix* for procedural details.

For roxadustat assays in mice, animals were treated with or without roxadustat (10 mg/kg daily i.p.) and/or oral Mn for 4 wk from ~4 wk of age. For these assays, animals received a higher level of Mn (~30 mg absolute Mn/kg daily) because exposure was initiated after weaning. Again, see *SI Appendix* for detailed procedures and justifications.

Cell Culture and Drug Treatments. HepG2 and 293T cells were cultured using standard procedures (details in *SI Appendix*). Human primary hepatocytes were obtained from XenoTech (catalog no. HPCH10+) and grown using procedures given by the supplier. The concentrations of drugs used in cell culture are provided in individual figure legends.

Lentiviral Infections. Luciferase constructs, dominant-negative plasmids, and shRNAs (sequences in *SI Appendix*, Table S3) were introduced into cells using a third-generation lentivirus system that we have described previously (49, 98).

Other Procedures. qRT-PCR (see *SI Appendix*, Table S4 for primer sequences), inductively coupled plasma mass spectrometry, neurobehavioral assays using the open-field test, immunofluorescence microscopy, cell viability assays, and immunoblots were performed essentially as described by us previously (47, 50, 51, 99). Luciferase assays were performed using the Luciferase Assay System Kit (Promega) and normalized to protein (Bio-Rad Protein Assay Dye, no. 5000006). The Prism 8 software (GraphPad) was used for statistical analyses. Statistical tests and sample size are provided in individual figure legends.

Data Availability. All study data are included in the article and/or *SI Appendix*.

1. E. Nemeth, T. Ganz, The role of hepcidin in iron metabolism. *Acta Haematol.* **122**, 78–86 (2009).

2. R. S. Polishchuk, E. V. Polishchuk, From and to the Golgi—Defining the Wilson disease protein road map. *FEBS Lett.* **593**, 2341–2350 (2019).

3. J. R. Forbes, D. W. Cox, Copper-dependent trafficking of Wilson disease mutant ATP7B proteins. *Hum. Mol. Genet.* **9**, 1927–1935 (2000).

4. S. Roy *et al.*, Analysis of Wilson disease mutations revealed that interactions between different ATP7B mutants modify their properties. *Sci. Rep.* **10**, 13487 (2020).

5. C. Casu, E. Nemeth, S. Rivella, Hepcidin agonists as therapeutic tools. *Blood* **131**, 1790–1794 (2018).

6. V. C. Culotta, M. Yang, M. D. Hall, Manganese transport and trafficking: Lessons learned from *Saccharomyces cerevisiae*. *Eukaryot. Cell* **4**, 1159–1165 (2005).

7. L. T. Jensen *et al.*, Down-regulation of a manganese transporter in the face of metal toxicity. *Mol. Biol. Cell* **20**, 2810–2819 (2009).

8. A. A. Britton, G. C. Cotzias, Dependence of manganese turnover on intake. *Am. J. Physiol.* **211**, 203–206 (1966).

9. G. C. Cotzias, J. J. Greenough, The high specificity of the manganese pathway through the body. *J. Clin. Invest.* **37**, 1298–1305 (1958).

10. P. S. Papavasiliou, S. T. Miller, G. C. Cotzias, Role of liver in regulating distribution and excretion of manganese. *Am. J. Physiol.* **211**, 211–216 (1966).

11. C. A. Taylor *et al.*, Maintaining translational relevance in animal models of manganese neurotoxicity. *J. Nutr.* **150**, 1360–1369 (2020).

12. B. A. Racette *et al.*, Increased risk of parkinsonism associated with welding exposure. *Neurotoxicology* **33**, 1356–1361 (2012).

13. M. Aschner, K. M. Erikson, E. Herrero Hernández, R. Tjalkens, Manganese and its role in Parkinson's disease: From transport to neuropathology. *Neuromolecular Med.* **11**, 252–266 (2009).

14. S. Y. Bhang *et al.*, Relationship between blood manganese levels and children's attention, cognition, behavior, and academic performance—A nationwide cross-sectional study. *Environ. Res.* **126**, 9–16 (2013).

15. M. Bouchard, F. Laforest, L. Vandelac, D. Bellinger, D. Mergler, Hair manganese and hyperactive behaviors: Pilot study of school-age children exposed through tap water. *Environ. Health Perspect.* **115**, 122–127 (2007).

16. M. F. Bouchard *et al.*, Intellectual impairment in school-age children exposed to manganese from drinking water. *Environ. Health Perspect.* **119**, 138–143 (2011).

17. B. Claus Henn *et al.*, Early postnatal blood manganese levels and children's neuro-development. *Epidemiology* **21**, 433–439 (2010).

18. K. Khan *et al.*, Manganese exposure from drinking water and children's classroom behavior in Bangladesh. *Environ. Health Perspect.* **119**, 1501–1506 (2011).

19. K. Khan *et al.*, Manganese exposure from drinking water and children's academic achievement. *Neurotoxicology* **33**, 91–97 (2012).

20. R. G. Lucchini *et al.*, Tremor, olfactory and motor changes in Italian adolescents exposed to historical ferro-manganese emission. *Neurotoxicology* **33**, 687–696 (2012).

21. Y. Oulhote *et al.*, Neurobehavioral function in school-age children exposed to manganese in drinking water. *Environ. Health Perspect.* **122**, 1343–1350 (2014).

22. H. Riojas-Rodríguez *et al.*, Intellectual function in Mexican children living in a mining area and environmentally exposed to manganese. *Environ. Health Perspect.* **118**, 1465–1470 (2010).

23. G. A. Wasserman *et al.*, Water manganese exposure and children's intellectual function in Araihazar, Bangladesh. *Environ. Health Perspect.* **114**, 124–129 (2006).

24. S. S. Kullar *et al.*, A benchmark concentration analysis for manganese in drinking water and IQ deficits in children. *Environ. Int.* **130**, 104889 (2019).

25. R. F. Butterworth, Parkinsonism in cirrhosis: Pathogenesis and current therapeutic options. *Metab. Brain Dis.* **28**, 261–267 (2013).

26. R. F. Butterworth, L. Spahr, S. Fontaine, G. P. Layrargues, Manganese toxicity, dopa-minergic dysfunction and hepatic encephalopathy. *Metab. Brain Dis.* **10**, 259–267 (1995).

27. G. Pomier-Layrargues, L. Spahr, R. F. Butterworth, Increased manganese concentrations in pallidum of cirrhotic patients. *Lancet* **345**, 735 (1995).

28. L. Spahr *et al.*, Increased blood manganese in cirrhotic patients: Relationship to pallidal magnetic resonance signal hyperintensity and neurological symptoms. *Hepatology* **24**, 1116–1120 (1996).

29. G. P. Layrargues, D. Shapcott, L. Spahr, R. F. Butterworth, Accumulation of manganese and copper in pallidum of cirrhotic patients: Role in the pathogenesis of hepatic encephalopathy? *Metab. Brain Dis.* **10**, 353–356 (1995).

30. C. Rose *et al.*, Manganese deposition in basal ganglia structures results from both portal-systemic shunting and liver dysfunction. *Gastroenterology* **117**, 640–644 (1999).

31. P. R. Burkhard, J. Delavelle, R. Du Pasquier, L. Spahr, Chronic parkinsonism associated with cirrhosis: A distinct subset of acquired hepatocerebral degeneration. *Arch. Neurol.* **60**, 521–528 (2003).

32. N. Ballatori, E. Miles, T. W. Clarkson, Homeostatic control of manganese excretion in the neonatal rat. *Am. J. Physiol.* **252**, R842–R847 (1987).

33. A. J. Bertinchamps, S. T. Miller, G. C. Cotzias, Interdependence of routes excreting manganese. *Am. J. Physiol.* **211**, 217–224 (1966).

34. C. D. Klaassen, Biliary excretion of manganese in rats, rabbits, and dogs. *Toxicol. Appl. Pharmacol.* **29**, 458–468 (1974).

35. D. M. Greenberg, D. H. Copp, E. M. Cuthbertson, Studies in mineral metabolism with the aid of artificial radioactive isotopes: VII. The distribution and excretion, particularly by way of the bile, of iron, cobalt, and manganese. *J. Biol. Chem.* **147**, 749–756 (1943).

36. K. Tuschl *et al.*, Mutations in SLC39A14 disrupt manganese homeostasis and cause childhood-onset parkinsonism-dystonia. *Nat. Commun.* **7**, 11601 (2016).

37. K. Tuschl *et al.*, Syndrome of hepatic cirrhosis, dystonia, polycythemia, and hyper-manganesemia caused by mutations in SLC30A10, a manganese transporter in man. *Am. J. Hum. Genet.* **90**, 457–466 (2012).

38. K. Tuschl *et al.*, Hepatic cirrhosis, dystonia, polycythaemia and hypermanganesaemia—A new metabolic disorder. *J. Inherit. Metab. Dis.* **31**, 151–163 (2008).

39. M. Quadri *et al.*, Mutations in SLC30A10 cause parkinsonism and dystonia with hy-permanganesemia, polycythemia, and chronic liver disease. *Am. J. Hum. Genet.* **90**, 467–477 (2012).

40. M. Lechpammer *et al.*, Pathology of inherited manganese transporter deficiency. *Ann. Neurol.* **75**, 608–612 (2014).

41. C. W. Olanow, Manganese-induced parkinsonism and Parkinson's disease. *Ann. N. Y. Acad. Sci.* **1012**, 209–223 (2004).

42. D. P. Perl, C. W. Olanow, The neuropathology of manganese-induced parkinsonism. *J. Neuropathol. Exp. Neurol.* **66**, 675–682 (2007).

43. D. S. Harischandra *et al.*, Manganese promotes the aggregation and prion-like cell-to-cell exosomal transmission of α-synuclein. *Sci. Signal.* **12**, eaau4543 (2019).

44. J. M. Gorell *et al.*, Occupational exposure to manganese, copper, lead, iron, mercury and zinc and the risk of Parkinson's disease. *Neurotoxicology* **20**, 239–247 (1999).

45. K. M. Boycott *et al.*, Autosomal-recessive intellectual disability with cerebellar atrophy syndrome caused by mutation of the manganese and zinc transporter gene SLC39A8. *Am. J. Hum. Genet.* **97**, 886–893 (2015).

46. J. H. Park *et al.*, SLC39A8 deficiency: A disorder of manganese transport and glyco-sylation. *Am. J. Hum. Genet.* **97**, 894–903 (2015).

47. D. Leyva-Illades *et al.*, SLC30A10 is a cell surface-localized manganese efflux transporter, and parkinsonism-causing mutations block its intracellular trafficking and efflux activity. *J. Neurosci.* **34**, 14079–14095 (2014).

48. C. E. Zogzas, M. Aschner, S. Mukhopadhyay, Structural elements in the transmembrane and cytoplasmic domains of the metal transporter SLC30A10 are required for its manganese efflux activity. *J. Biol. Chem.* **291**, 15940–15957 (2016).

49. C. E. Zogzas, S. Mukhopadhyay, Putative metal binding site in the transmembrane domain of the manganese transporter SLC30A10 is different from that of related zinc transporters. *Metallomics* **10**, 1053–1064 (2018).

50. C. Liu *et al.*, Hypothyroidism induced by loss of the manganese efflux transporter SLC30A10 may be explained by reduced thyroxine production. *J. Biol. Chem.* **292**, 16605–16615 (2017).

51. C. A. Taylor *et al.*, SLC30A10 transporter in the digestive system regulates brain manganese under basal conditions while brain SLC30A10 protects against neuro-toxicity. *J. Biol. Chem.* **294**, 1860–1876 (2019).

52. C. J. Mercadante *et al.*, Manganese transporter Slc30a10 controls physiological manganese excretion and toxicity. *J. Clin. Invest.* **129**, 5442–5461 (2019).

53. R. C. Balachandran *et al.*, Brain manganese and the balance between essential roles and neurotoxicity. *J. Biol. Chem.* **295**, 6312–6329 (2020).

54. S. Jenkitkasemwong, C. Y. Wang, B. Mackenzie, M. D. Knutson, Physiologic implications of metal-ion transport by ZIP14 and ZIP8. *Biometals* **25**, 643–655 (2012).

55. T. B. Aydemir *et al.*, Metal transporter *Zip14* (*Slc39a14*) deletion in mice increases manganese deposition and produces neurotoxic signatures and diminished motor activity. *J. Neurosci.* **37**, 5996–6006 (2017).

56. S. Jenkitkasemwong *et al.*, SLC39A14 deficiency alters manganese homeostasis and excretion resulting in brain manganese accumulation and motor deficits in mice. *Proc. Natl. Acad. Sci. U.S.A.* **115**, E1769–E1778 (2018).

57. Y. Xin *et al.*, Manganese transporter Slc39a14 deficiency revealed its key role in maintaining manganese homeostasis in mice. *Cell Discov.* **3**, 17025 (2017).

58. I. F. Scheiber, Y. Wu, S. E. Morgan, N. Zhao, The intestinal metal transporter ZIP14 maintains systemic manganese homeostasis. *J. Biol. Chem.* **294**, 9147–9160 (2019).

59. T. B. Aydemir *et al.*, Intestine-specific deletion of metal transporter *Zip14* (*Slc39a14*) causes brain manganese overload and locomotor defects of manganism. *Am. J. Physiol. Gastrointest. Liver Physiol.* **318**, G673–G681 (2020).

60. W. Lin *et al.*, Hepatic metal ion transporter ZIP8 regulates manganese homeostasis and manganese-dependent enzyme activity. *J. Clin. Invest.* **127**, 2407–2417 (2017).

61. J. Jeong, D. J. Eide, The SLC39 family of zinc transporters. *Mol. Aspects Med.* **34**, 612–619 (2013).

62. B. D. Semple, K. Blomgren, K. Gimlin, D. M. Ferriero, L. J. Noble-Haeusslein, Brain development in rodents and humans: Identifying benchmarks of maturation and vulnerability to injury across species. *Prog. Neurobiol.* **106–107**, 1–16 (2013).

63. S. Mukhopadhyay, A. D. Linstedt, Identification of a gain-of-function mutation in a Golgi P-type ATPase that enhances Mn2+ efflux and protects against toxicity. *Proc. Natl. Acad. Sci. U.S.A.* **108**, 858–863 (2011).

64. O. Bensaude, Inhibiting eukaryotic transcription: Which compound to choose? How to evaluate its activity? *Transcription* **2**, 103–108 (2011).

65. D. Farré *et al.*, Identification of patterns in biological sequences at the ALGGEN server: PROMO and MALGEN. *Nucleic Acids Res.* **31**, 3651–3653 (2003).

66. X. Messeguer *et al.*, PROMO: Detection of known transcription regulatory elements using species-tailored searches. *Bioinformatics* **18**, 333–334 (2002).

67. P. Schummer, S. Kuphal, L. Vardimon, A. K. Bosserhoff, M. Kappelmann, Specific c-Jun target genes in malignant melanoma. *Cancer Biol. Ther.* **17**, 486–497 (2016).

68. L. Chen *et al.*, Genome-wide analysis of YY2 versus YY1 target genes. *Nucleic Acids Res.* **38**, 4011–4026 (2010).

69. X. Zhao *et al.*, Mechanisms involved in the activation of C/EBPα by small activating RNA in hepatocellular carcinoma. *Oncogene* **38**, 3446–3457 (2019).

70. J. Kim *et al.*, Wild-type p53 promotes cancer metabolic switch by inducing PUMA-dependent suppression of oxidative phosphorylation. *Cancer Cell* **35**, 191–203.e8 (2019).

71. S. Y. Cai, H. He, T. Nguyen, A. Mennone, J. L. Boyer, Retinoic acid represses CYP7A1 expression in human hepatocytes and HepG2 cells by FXR/RXR-dependent and independent mechanisms. *J. Lipid Res.* **51**, 2265–2274 (2010).

72. A. J. Majmundar, W. J. Wong, M. C. Simon, Hypoxia-inducible factors and the response to hypoxic stress. *Mol. Cell* **40**, 294–309 (2010).

73. D. R. Mole *et al.*, Genome-wide association of hypoxia-inducible factor (HIF)-1alpha and HIF-2alpha DNA binding with expression profiling of hypoxia-inducible transcripts. *J. Biol. Chem.* **284**, 16767–16775 (2009).

74. W. G. Kaelin, Proline hydroxylation and gene expression. *Annu. Rev. Biochem.* **74**, 115–128 (2005).

75. M. Hirsilä, P. Koivunen, V. Günzler, K. I. Kivirikko, J. Myllyharju, Characterization of the human prolyl 4-hydroxylases that modify the hypoxia-inducible factor. *J. Biol. Chem.* **278**, 30772–30780 (2003).

76. Q. Li, H. Chen, X. Huang, M. Costa, Effects of 12 metal ions on iron regulatory protein 1 (IRP-1) and hypoxia-inducible factor-1 alpha (HIF-1alpha) and HIF-regulated genes. *Toxicol. Appl. Pharmacol.* **213**, 245–255 (2006).

77. K. Salnikow *et al.*, Depletion of intracellular ascorbate by the carcinogenic metals nickel and cobalt results in the induction of hypoxic stress. *J. Biol. Chem.* **279**, 40337–40344 (2004).

78. T. L. Davidson, H. Chen, D. M. Di Toro, G. D'Angelo, M. Costa, Soluble nickel inhibits HIF-prolyl-hydroxylases creating persistent hypoxic signaling in A549 cells. *Mol. Carcinog.* **45**, 479–489 (2006).

79. P. Maxwell, K. Salnikow, HIF-1: An oxygen and metal responsive transcription factor. *Cancer Biol. Ther.* **3**, 29–35 (2004).

80. J. Han *et al.*, Manganese (II) induces chemical hypoxia by inhibiting HIF-prolyl hydroxylase: Implication in manganese-induced pulmonary inflammation. *Toxicol. Appl. Pharmacol.* **235**, 261–267 (2009).

81. N. Ohgami *et al.*, Manganese-mediated acceleration of age-related hearing loss in mice. *Sci. Rep.* **6**, 36306 (2016).

82. K. Lee *et al.*, LW6, a novel HIF-1 inhibitor, promotes proteasomal degradation of HIF-1alpha via upregulation of VHL in a colon cancer cell line. *Biochem. Pharmacol.* **80**, 982–989 (2010).

Liu et al.
Up-regulation of the manganese transporter SLC30A10 by hypoxia-inducible factors defines a homeostatic response to manganese toxicity

PNAS | 11 of 12
https://doi.org/10.1073/pnas.2107673118

83. N. S. Sanghani, V. H. Haase, Hypoxia-inducible factor activators in renal anemia: Current clinical experience. *Adv. Chronic Kidney Dis.* **26**, 253–266 (2019).

84. A. Besarab *et al.*, Roxadustat (FG-4592): Correction of anemia in incident dialysis patients. *J. Am. Soc. Nephrol.* **27**, 1225–1233 (2016).

85. P. E. Pergola, B. S. Spinowitz, C. S. Hartman, B. J. Maroni, V. H. Haase, Vadadustat, a novel oral HIF stabilizer, provides effective anemia treatment in nondialysis-dependent chronic kidney disease. *Kidney Int.* **90**, 1115–1122 (2016).

86. Z. L. Li, Y. Tu, B. C. Liu, Treatment of renal anemia with roxadustat: Advantages and achievement. *Kidney Dis.* **6**, 65–73 (2020).

87. C. M. Wade, M. J. Daly, Genetic variation in laboratory mice. *Nat. Genet.* **37**, 1175–1180 (2005).

88. J. Lilue *et al.*, Sixteen diverse laboratory mouse reference genomes define strain-specific haplotypes and novel functional loci. *Nat. Genet.* **50**, 1574–1583 (2018).

89. A. Yoshiki, K. Moriwaki, Mouse phenome research: Implications of genetic background. *ILAR J.* **47**, 94–102 (2006).

90. X. Montagutelli, Effect of the genetic background on the phenotype of mouse mutations. *J. Am. Soc. Nephrol.* **11** (suppl. 16), S101–S105 (2000).

91. R. E. Fleming *et al.*, Mouse strain differences determine severity of iron accumulation in Hfe knockout model of hereditary hemochromatosis. *Proc. Natl. Acad. Sci. U.S.A.* **98**, 2707–2711 (2001).

92. B. L. Ebert, H. F. Bunn, Regulation of the erythropoietin gene. *Blood* **94**, 1864–1877 (1999).

93. K. Wahlberg *et al.*, Common polymorphisms in the solute carrier SLC30A10 are associated with blood manganese and neurological function. *Toxicol. Sci.* **149**, 473–483 (2016).

94. K. E. Wahlberg *et al.*, Polymorphisms in manganese transporters *SLC30A1*0 and *SLC39A8* are associated with children's neurodevelopment by influencing manganese homeostasis. *Front. Genet.* **9**, 664 (2018).

95. T. R. Ahmad *et al.*, Bile acid composition regulates the manganese transporter Slc30a10 in intestine. *J. Biol. Chem.* **295**, 12545–12558 (2020).

96. T. Claro da Silva, C. Hiller, Z. Gai, G. A. Kullak-Ublick, Vitamin D3 transactivates the zinc and manganese transporter SLC30A10 via the vitamin D receptor. *J. Steroid Biochem. Mol. Biol.* **163**, 77–87 (2016).

97. S. Li *et al.*, Analysis of 1,25-dihydroxyvitamin D_3 genomic action reveals calcium-regulating and calcium-independent effects in mouse intestine and human enteroids. *Mol. Cell. Biol.* **41**, e00372-20 (2020).

98. A. S. Selyunin, L. R. Iles, G. Bartholomeusz, S. Mukhopadhyay, Genome-wide siRNA screen identifies UNC50 as a regulator of Shiga toxin 2 trafficking. *J. Cell Biol.* **216**, 3249–3262 (2017).

99. S. Hutchens *et al.*, Deficiency in the manganese efflux transporter SLC30A10 induces severe hypothyroidism in mice. *J. Biol. Chem.* **292**, 9760–9773 (2017).

Liu et al.

Up-regulation of the manganese transporter SLC30A10 by hypoxia-inducible factors defines a homeostatic response to manganese toxicity